CZECH TECHNICAL UNIVERSITY IN PRAGUE

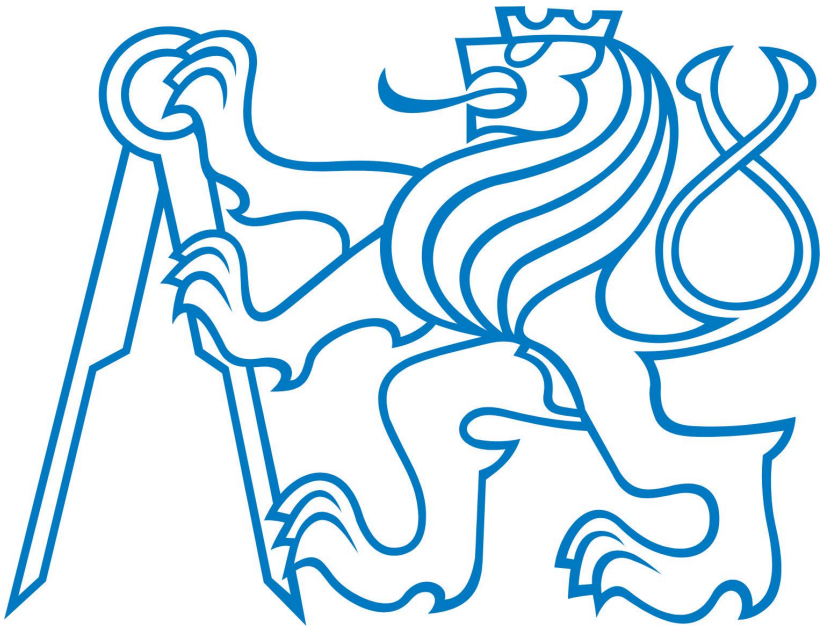

DOCTORAL THESIS STATEMENT

Czech Technical University in Prague

Faculty of Electrical Engineering

Department of Electromagnetic Field

Petr Dvořák

NEW METHODOLOGIES OF REMOTE SENSING BASED ON MICROWAVE RADIOMETER

Ph.D. Programme:
Electrical Engineering and Information Technology

Branch of study: Radioelectronics

Doctoral thesis statement for obtaining the academic title of "Doctor", abbreviated to "Ph.D."

Prague, February 2014

The doctoral thesis was produced in full-time manner Ph.D. study at the department of electromagnetic field of the Faculty of Electrical Engineering of the CTU in Prague

Candidate: Ing. Petr Dvořák

Department of Electromagnetic Field
Faculty of Electrical Engineering of the CTU in Prague
Technická 2, 166 27 Prague 6

Supervisor: Prof. Ing. Miloš Mazánek, CSc.

Department of Electromagnetic Field
Faculty of Electrical Engineering of the CTU in Prague
Technická 2, 166 27 Prague 6

Supervisor-Specialist: Doc. Ing. Stanislav Zvánovec, Ph.D.

Department of Electromagnetic Field
Faculty of Electrical Engineering of the CTU in Prague
Technická 2, 166 27 Prague 6

Opponents:

The doctoral thesis statement was distributed on:

The defence of the doctoral thesis will be held on ..... at ..... a.m./p.m. before the Board for the Defence of the Doctoral Thesis in the branch of study Radioelectronics in the meeting room No. ..... of the Faculty of Electrical Engineering of the CTU in Prague.

Those interested may get acquainted with the doctoral thesis concerned at the Dean Office of the Faculty of Electrical Engineering of the CTU in Prague, at the Department for Science and Research, Technická 2, Praha 6.

Chairman of the Board for the Defence of the Doctoral Thesis
in the branch of study Radioelectronics
Faculty of Electrical Engineering of the CTU in Prague
Technická 2, 166 27 Prague 6

CURRENT SITUATION OF THE STUDIED PROBLEM

Remote sensing methods have been and continue to be developed over the last few decades with rapidly increasing technical maturity. Throughout history, the surrounding world was perceived using simple methods whereby humans interacted directly with nature. Short-range fields (temperature, acoustic) were observed and investigated, and subsequent attempts to make sense of the observations focused on objects more and more remote from the Earth's atmosphere such as planets and stars rather than the closest space object, the Moon. Since direct sensing of these objects is either extremely difficult or impossible, it is only by measuring long-range fields that these remote objects can be effectively examined.

One of the first remote sensing attempts was done by Gaspard-Félix Tournachon. Tournachon first made pictures of Earth, essentially Paris, from a balloon. Since that time, 1858, when the images of Paris were distributed, mankind has gone on to such bold and daunting projects such as the launching of the Planck probe, in 2009, by the European Space Agency [1]. The probe is equipped with state-of-the-art radiometers which scan the temperature of the universe in three frequency bands from 30 GHz to 70 GHz [2].

The electromagnetic field is the most convenient means of conducting remote sensing and most widely used for sensing a wide-frequency spectrum allows scientists to observe the object from various points of view – in terms of sensing various states and process by one quantity.

Currently, new types of radiometers have been developed allowing us to integrate them with more complex measurement systems. Together, with the miniaturization of radiometric systems thanks to MEMS devices and system-on-chip technologies, radiometry boasts a new perspective for remote sensing from satellite, airborne or ground-based scanning.

New methodologies of remote sensing will be described in this thesis. Since the instrumentation for remote sensing is accessible and well developed, opportunities to propose new methodologies of measuring and datamining that are crucial in current research abound.

The main aim of this doctoral thesis is to propose new methodologies of remote sensing. The thesis is focused on currently used radiometric methodologies in remote sensing of the terrestrial atmosphere, and, fire detection and localization. The thesis is organized as follows. Following the introduction a theoretical background of remote sensing is introduced in the second chapter; Principles and fundamental laws are explained first with currently used radiometeric concepts also being presented. In the third chapter, state-of-the-art remote sensing is discussed with general methodologies of ground-based atmosphere sensing highlighted, followed by a discussion of measuring atmospheric profiles. In relation to atmospheric profiles, precipitation detection and prediction is discussed. The second part of the third chapter is focused on methods of fire detection. In the fourth chapter the thesis objectives are proposed and defined. The main thesis focus consists of two parts: the first part deals with the new methodology of atmosphere dynamic effects (rain, clouds) sensing and the next chapter describes the methodology of remote fire detection and its properties from a microwave point of view.

Ground Based Sensing of Atmosphere

Passive atmosphere sensing is mainly performed in the visible part of the spectrum, as well as in infrared and radiofrequency bands. Visible and infrared waves radiated upwards from clouds are often reflected and emitted by top cloud layers and insufficiently correlated to the microphysical structure of clouds below the top layer. This is the reason why the visible/infrared information cannot be used satisfactorily for rain detection and prediction. Clouds are mainly related to rainfall in convective systems.

Precipitation Sensing

Having an atmosphere model and profiles, precipitation sensing and prediction can be investigated. In 1999 J. Guldner performed water vapor sensing via a ground-based radiometer over a 1-year

period. Guldner proposed findings from measuring precipitable water vapor (PWV) and cloud liquid water (CLW) [3]. The data were measured in central Europe.

A pure state of the art precipitation detection and prediction model by a microwave ground-based radiometer was performed by H. Y. Won [4]. To estimate rainfall occurrence and intensity, a ground based microwave radiometer was used. Ordinary upper-air observation provided by a radioprobe 2 times a day cannot satisfactory substitute local on-line monitoring recording short-time precipitations. By statistical evaluation of measured brightness temperature, Guldner measured PWV and CLW increase of in a 30 minute time interval of before the rain started. Guldner measured the brightness temperature at two channels, 23.8 GHz and 31.4 GHz respectively.

In the Gueldner's work Won continues with his precipitation prediction by a ground-based radiometer [4]. Won has used microwave radiometer that measures 8 water vapor channels in the K-band and 14 oxygen channels in the V-band.

Predictability of precipitation events can be proved by using 15-minute moving data accumulation. If in the 15-minute interval a statistically significant rainfall is detected, it is considered as the rain event.

Typical results of Won's method are depicted in Fig. 1. In figures averaged differences of brightness temperature in period of 2 h before the rain starts can be seen. The difference of RR and NR graphs is obvious.

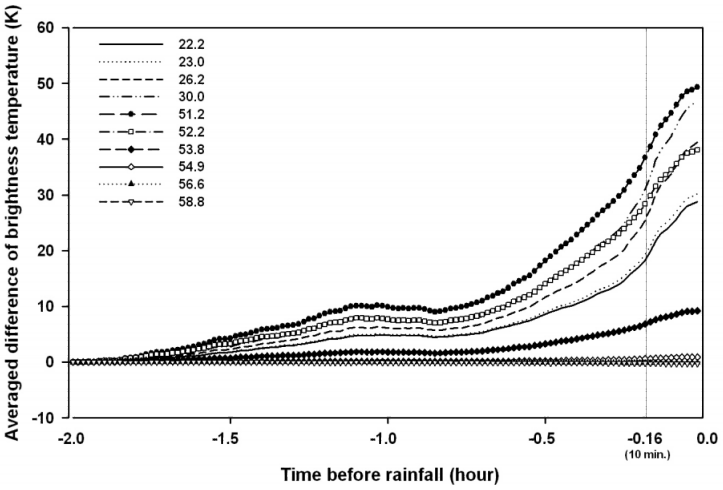

Figure 1: Time averaged brightness temperature differences in 2-hour period before the rain event. RR datasets measured at water vapor frequency channels are used [4].

Methods of Remote Sensing in Case of Fires

As well as the atmosphere can be explored in order to detect and predict undesirable atmospheric effects, fires can be sensed by measuring of thermal radiation too. Every year thousands of square kilometers are burned out because of forest fires causing huge damages on environment and human health. A various fires can be distinguished: fires in buildings, open space fires, fires of dangerous chemical etc. In order to detect fire many way exists where radiometry is one of the interesting tool for this purpose. Currently used fire detectors, from remote sensing point of view, are based on satellite infrared sensors. The problem of infrared sensors is in possible miss of the fire hidden under a vegetation or other coverage. Since microwaves can penetrate the vegetation layer, which is opaque for visible or IR radiation, radiometers can be successfully used.

Fires Detection

As well as the atmosphere being studied to detect and predict undesirable atmospheric effects, fires can be sensed by measuring thermal radiation too. Every year thousands of square kilometers are

destroyed by forest fires causing huge damage to the environment and people. A variety of fires can be distinguished: fires in buildings, open space fires, fires of dangerous chemicals etc. Detecting fire by radiometry has great potential. Current fire detectors, from a remote sensing point of view, are based on infrared satellite sensors, though problems exist as infrared sensors may not detect fire hidden under vegetation or other forms of coverage. Since microwaves can penetrate the vegetation layer, which is opaque for visible or IR radiation, radiometers can be successfully used.

Radiometers for the purpose of fire detection are well designed by the group of F. Alimenti. Alimenti has designed several radiometers for various purposes [5, 6, 7, 8] and the ability to detect a fire was proved. The ability of fire detection was performed by measuring of the open wood fire. For this purpose the microwave radiometer was developed. The working frequency was 12.65 GHz with the bandwidth of 100 MHz. A low-cost radiometer was used to measure thermal radiation in accordance with the European standard EN54. The standard is used to certify optical and temperature fire detectors. The standard alse describes the fire sizes and types in order to simulate the wild fires etc. Materials of the fuel is mentioned as well. In Fig. 2 the course of experiment is depicted.

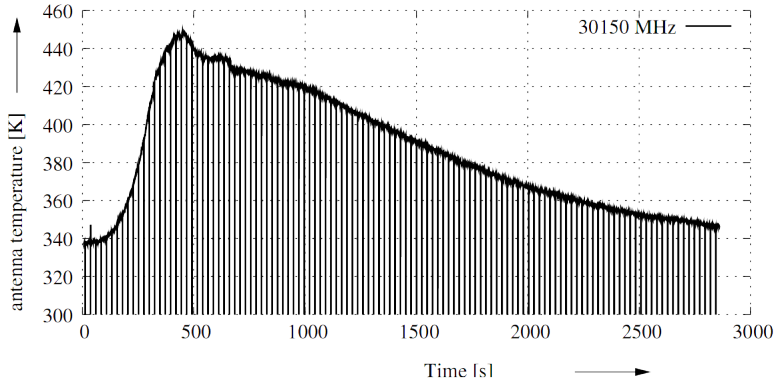

Figure 2: Measured brightness temperature of a wood fire. Experimental procedure performed to prove ability of fire detection in accordance with EN54 standard. The signal dropouts are caused by the radiometer calibration [6].

The brightness temperature increase was from 0.2 dB to 1.5 dB for various solid fuels used in the experiment. No dependency of the used frequency in the range of chosen band was observed. Thus, there is no strong requirement on the frequency band. Also the brightness temperature differences are more important than the absolute value of temperature so the calibration of the radiometer is not essential in this application.

AIMS OF THE DOCTORAL THESIS

The doctoral thesis proposes new methodologies of microwave radiometric sensing. Since a lot of atmospheric and environmental effects decrease reliability of newly planned wireless links or sensors (either microwave or optical) and with recent advances in radiometer technology (e.g. miniaturized MEMS based radiometers which allow to construct small, cheap and portable radiometric devices), new algorithms for undesirable effects detection and prediction have to be proposed. Two main objectives will be solved.

I The thesis will be primary focused mostly on derivation of methodologies for prediction and detection of dynamic atmospheric changes relating to rains. In order to obtain statistically significant amount of measured data, a measuring campaign will be accomplished. Specific atmospheric effects, e.g. cloudiness and precipitation, will be analyzed based on samples of brightness temperatures. A methodology to predict and detect rain events, and clouds from brightness temperature dependencies will be proposed and verified.

II Each summer thousands of square kilometers of forests are burned out with huge impact on both environment and economy. Precise detection and localization of fires is a contemporary well demanded service in order to secure human lives and assets. In order to improve the detection and localization of fires, microwave radiometers can be used for the ground scanning. In comparison of radiometer with IR camera the microwave instrumentation brings the advantage to sense even through obstacles or smoke. In the second aim of the thesis, the detectability of a particular fire types by aerial microwave radiometer will be investigated with respect to specific parameters like the fire size, temperature and especially radiometer sensitivity. There are a few papers published about the fire sensing topic but mainly focused on hardware development and not on methodologies of measurement approaches and data processing. Several measurements will be performed in order to study the fire from the radiometric point of view and a new methodology will be described.

WORKING METHODS: Atmosphere Sensing

In order to validate brightness temperature changes and to obtain better statistical insight, an experimental site was set up in the university campus of the Faculty of Electrical Engineering, Czech Technical University in Prague (CTU), Czech Republic. The experimental measuring system consists of a ground based radiometric station and a set of weather sensors located at two meteorological stations.

The microwave radiometer based on the Dicke switch design [9] was utilized for long-term monitoring of brightness temperature. The lower working frequency range of 10.68 to 11.49 GHz (satellite band) was chosen to measure the thermal deviation for two main reasons - we wanted to avoid the strong absorption line of water vapor in the atmosphere at 22.2 GHz, which would cause partial biasing of measurement results, and secondly because the technology for satellite receivers was available. Using frequency band lower than 37 GHz leads to measurements of the brightness temperature that responds more to rain or cloud liquid emissions. Contrary to band with frequencies higher than 37 GHz, where brightness temperature mainly responds to cloud ice scattering [10].

The vertically pointed radiometer was deployed on the roof of the CTU building, 36 m above the ground level, therefore it was isolated with respect to the brightness temperature contribution in a given antenna (receiving) radiation pattern of received noise signal from adjacent buildings.

As a receiving antenna the parabolic reflector antenna with the diameter of 64 cm was used.

The radiometer exterior and internal deployments are shown in Fig. 3 – the parabolic antenna of the radiometer points vertically through a planar metal mirror tilted under angle of 45 °.

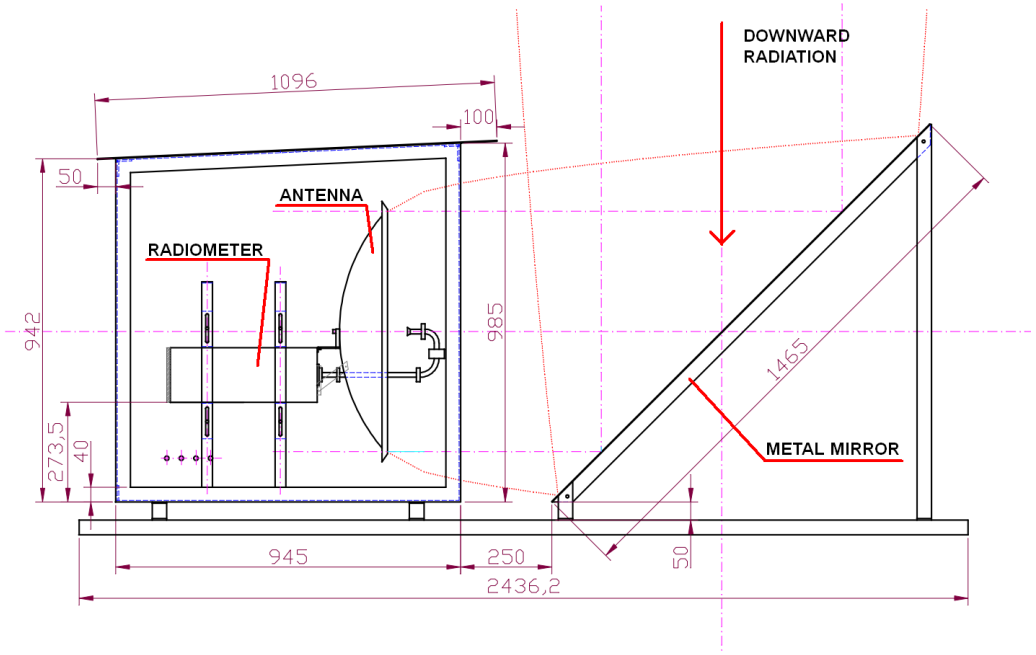

Figure 3: Radiometer deployment: Schematic view and dimensions.

This arrangement was chosen in order to avoid antenna aperture deformation by any obstacles (like snow, rain water) on the upper cover that could affect precision of measurement. The metal surface of the mirror was also smeared with a hydrophobic film of silicon oil in order to trickle water drops away. The chosen arrangement allows to measure brightness temperature of the ice and liquid content of clouds in the vertical direction. The main radiometric system parameters are listed in table 1.

Table 1: Radiometric system parameters.

Parameter	Value
Radiometer bandwidth	0.81 GHz
Integration time	0.5 ms
Radiometer sensitivity	0.7 K
Antenna beamwidth (-3 dB)	4.4 deg
Sidelobe suppression	>20 dB
Measuring data averaging interval	3 s
GPS location	50.10339, 14.392749

Data from two (primary and backup) meteorological stations WS981, made by the Anemo Corporation, Czech Republic [11], have been used for further analysis. Each station collects the temperature and humidity, as well as atmospheric pressure (barometer TMAG 518N4F with range 800 - 1200 hPa), precipitations (heated tipping-bucket rain gauge with a collecting area of 500 cm^2, and the rain amount per one tip of 0.1 mm), and the speed and direction of the wind (anemometer AN 955C). The primary meteorological station is located at same place as the radiometer, i.e. 36 m above ground level. Measurement data are collected in 1 minute intervals, therefore to harmonize the sampling of meteorological and radiometer data, the 3 second intervals of radiometer data were averaged over 1 minute. Only measurements of temperature and precipitation were used for direct processing.

RESULTS: Atmosphere Sensing

Method for Precipitation Prediction

In this section, the relation between measured brightness temperature and weather conditions will be discussed.

Measured data were analyzed over the period of 14 months, from March 2010 to April 2011. During this period 314 clearly defined atmospheric states were observed. These states can be detected or predicted by a microwave radiometer with the use of the proper statistical tools. To achieve the best results the method with variance enumeration was proposed.

The main aim of the paper is to introduce the detection of dynamic atmospheric events that are connected with certain atmospheric states. Initially, the utilization of a microwave radiometer as a precipitation detector and especially for precipitation prediction was investigated.

A simple approach using a steady threshold to predict rain events [12] was dismissed at the beginning of analysis because it had led to a higher number of "False alarms". In Fig. 4 a typical situation is depicted on the set of precipitation and brightness temperature data. In this simple (generally used) steady threshold method of cloud or rain event detection, a particular threshold is first carefully determined. When the brightness temperature exceeds the threshold limit, an event is predicted (Hit indication). The main problem arises with the threshold determination. When a low threshold is chosen to achieve extremely sensitive forecasting (i.e. for radiometer measurements in time intervals shorter than 1 minute), a number of "False alarm" signals are usually generated. By establishing a higher threshold we can on the one hand rapidly reduce the number of false alarms, but on the other hand, as it was confirmed by our analyses, this causes more "Misses" and, what is more, it inconveniently shortens the forecasting period before events. In other words, in many cases it results in the degradation of forecasting information. An example of false alarm signals observed on 24th May 2010 before 12.00 (note: all measurement records are related to UTC) can be distinguished in Fig. 4. In this case, the threshold was set to a value of 80 K of brightness temperature.

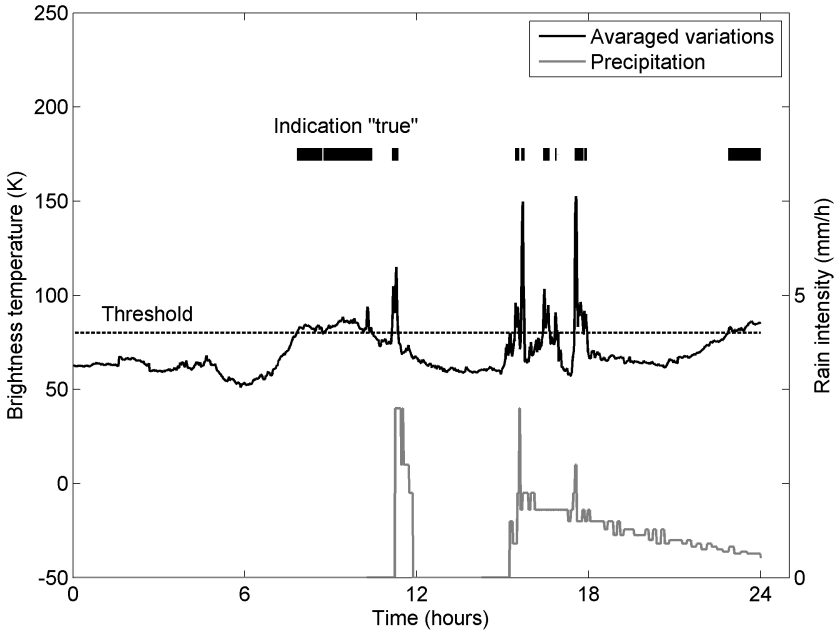

Figure 4: Example of simple threshold method utilization for the prediction of rain events; data from 24th of May 2010.

Since the success rate of the method analyzed above had not proved satisfactory, a more reliable detecting method based on observations that the rapid increase of brightness temperature precedes

rain events was proposed. The new method inheres in brightness temperature variances calculated over a particular time window within the measuring period. By parametric study, a 5 minute window of variance calculation was found to be the most effective. A shorter window results in higher variances even for non-significant events e.g. an artificial ripple in the brightness temperature, while with a longer window the forecasting information degrades or is lost. To smooth the variance curve, an additional moving average over the 15 minute time window can be applied (note this is not as significant as the first moving average to obtain variances, the 15 minute interval was optimized based on measured data). After these operations the detection threshold can be determined. The advantage of using the variances in this method is in the obvious suppression of slow brightness temperature changes. In this way, variance is also free from the absolute value of measured brightness temperature. The same situation as in Fig. 4 is newly demonstrated in Fig. 5, where the threshold was applied to the curve obtained by moving-averaged variances. It can clearly be seen that false alarm signals were suppressed, and only real rain events could be detected in advance without a significant number of false signals.

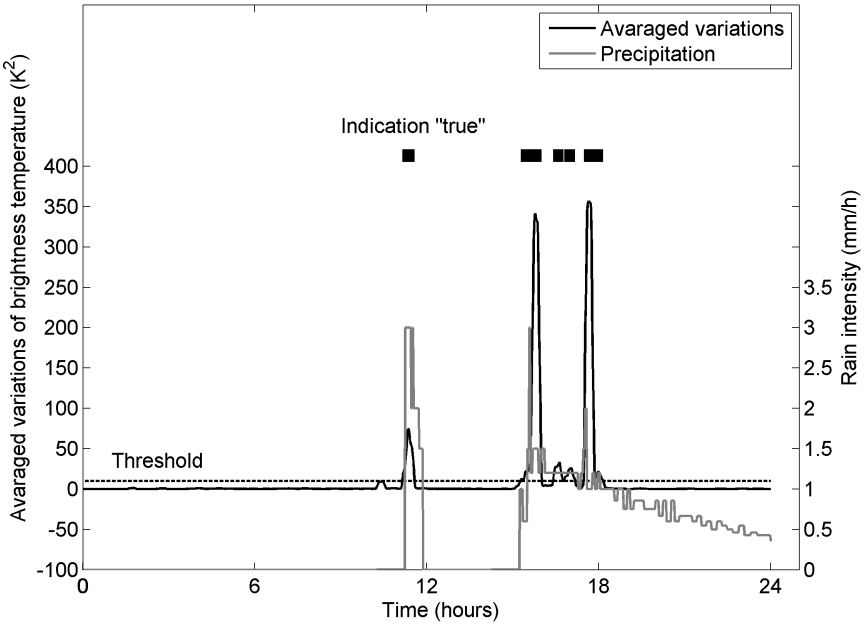

Figure 5: Example of undesirable signals suppression and rain prediction by using the method proposed in this contribution; data from 24th May 2010.

The probability of the successful utilization (hit rate) of the proposed method applied to the whole data set (314 events were considered) is summarized in Tab. 2. The whole range of temperature variations thresholds was scanned and the optimum of 10 K was determined as the value corresponding to the highest and the most stable hit rate over the evaluated period.

To determine the average forecasting time before rain detection at ground level (note this can be for short intervals more precisely expressed as a detection time), a cross-correlation function was used. Every pattern of events was correlated to the function processed for forecasting (variation, averaging) and the correlation was calculated for different time shifts. The maximum of the cross-correlation product and corresponding forecasting time was derived (see Fig. 6). The average time of the event forecast before the start of precipitation is 1.8 minutes. Since the variance is calculated over a moving time window of measured data, the result of averaging is delayed to brightness temperature changes. Note that the real peaks of brightness temperature can be observed quite some time before the start of rain (approximately 5 – 10 minutes). The forecasting time of 1.8 minutes represents a compromise value and corresponds to an acceptable number of Hits and False alarms. There is also a certain degree of freedom, and therefore it is possible to choose between a relatively improved

Table 2: Hit rate of precipitation forecasting by the proposed method.

Threshold	Event Forecast		
	Yes		No
	Event Observation		Event Observation
	Yes	No	Yes
8 K	75,4 %	11,7 %	12,9 %
9 K	75,1 %	11,4 %	13,6 %
10 K	74,4 %	7,7 %	17,9 %
11 K	70,1 %	7,5 %	22,4 %
12 K	59,5 %	7,3 %	33,2 %

forecasting time, but at the cost of a higher number of False alarms or Missed events. The forecasting time is shortened because of the averaging.

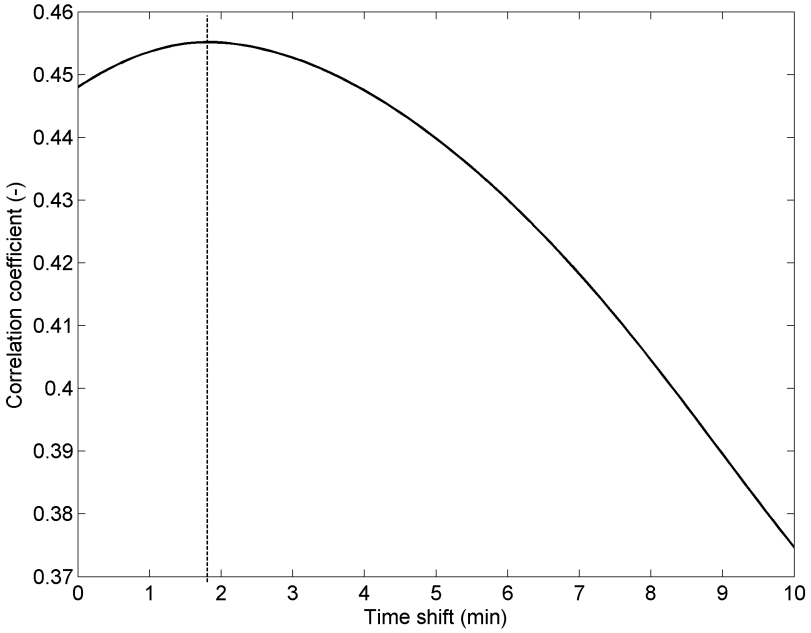

Figure 6: Averaged cross-correlation products of all rain events.

Method for Cloud Detection

Next the cloudiness detection method will be described. After eliminating the influence of rain, brightness temperature measured by the microwave radiometer and meteorological data was further analyzed. Despite a high randomness rate in the meteorological data, some particularly interesting relationships were observed. At first, the brightness temperature varied from 47 K up to 65 K, even during periods of clear skies. The amplitude of the measured brightness temperature was dependent on sunshine, i.e. in the daytime. Almost all the higher brightness temperatures with more rapid brightness temperature changes were related to specific types of cloudiness [13] (for cloudiness types see [14]). These issues were also partially described by Long in [15].

For cloudiness detection, a similar technique was used as for precipitation prediction. This method exploits the instability of brightness temperature when a cloud moves through the observed volume. Again, the variance of the brightness temperature was calculated within a 5minute time window over the entire period.

A typical behavior pattern for brightness temperature is depicted in Fig. 7, where the clouds presence in the monitored volume of atmosphere from 7.00 to 18.00 caused higher variations of the brightness temperature.

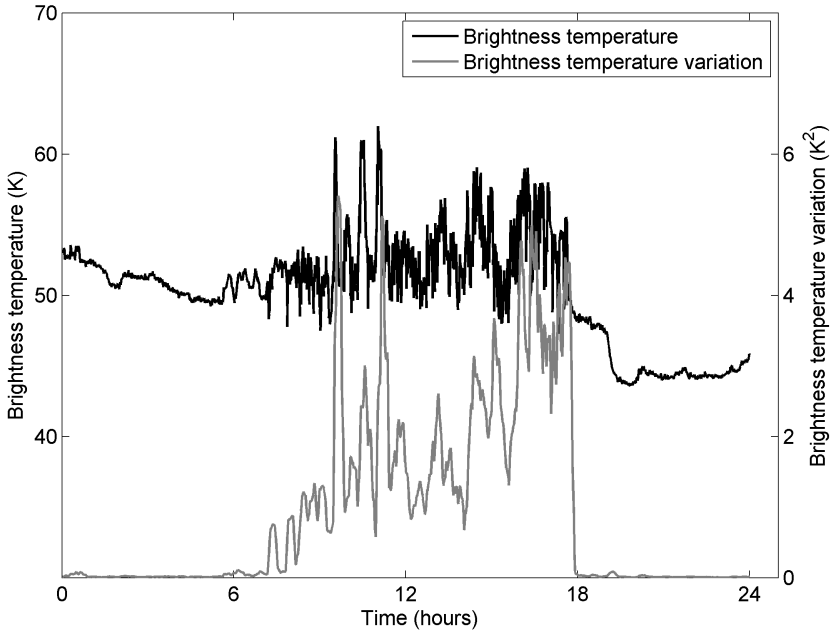

Figure 7: Typical variations of the brightness temperature during clouds presence in the monitored volume of atmosphere on 5th April 2010.

Variations of brightness temperature are depicted as a function of ambient temperature in Fig. 8 (156 events were captured). The incidence of low temperature can be observed. From the measurements it was found that when the ambient temperature is above 0 °C, the variation of brightness temperature due to the cloud presence is higher - in the range from 0.2 to 4 K. It should be emphasized that when the ambient temperature is below 0 °C, the variation ranges from 0 to 0.5 K. The temperature at ground level (measured by the weather station) is highly correlated to the temperature in the monitored volume of atmosphere above (obtained from the radiometer). Since the radiometer is thermally stabilized, possible slow and minor temperature deviations cannot significantly affect the measurements. To ensure correct interpretation of the results, the influence of temperature (below/above 0) is considered and the results are described for both temperature ranges.

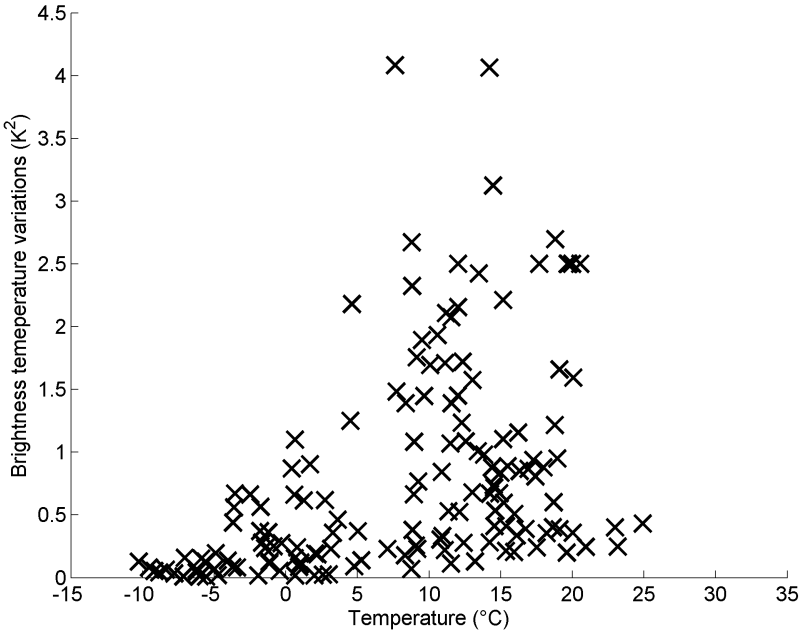

Figure 8: Brightness temperature variations when clouds passed through the vertical volume monitored by the radiometer.

In Fig. 9, variation of brightness temperature is shown in a cloudless situation in the monitored volume of atmosphere – 158 events were captured during the cloudless period. The contrast with the cloudy case (Fig. 8) is obvious. The variation does not exceed the value of 0.25 K during the cloudless period. Variations, based on measurements when clouds were in the observed volume, can be clearly separated from the state when no clouds were present in the observed volume, and hence a method to detect cloudiness based on the calculation of variations can be proposed.

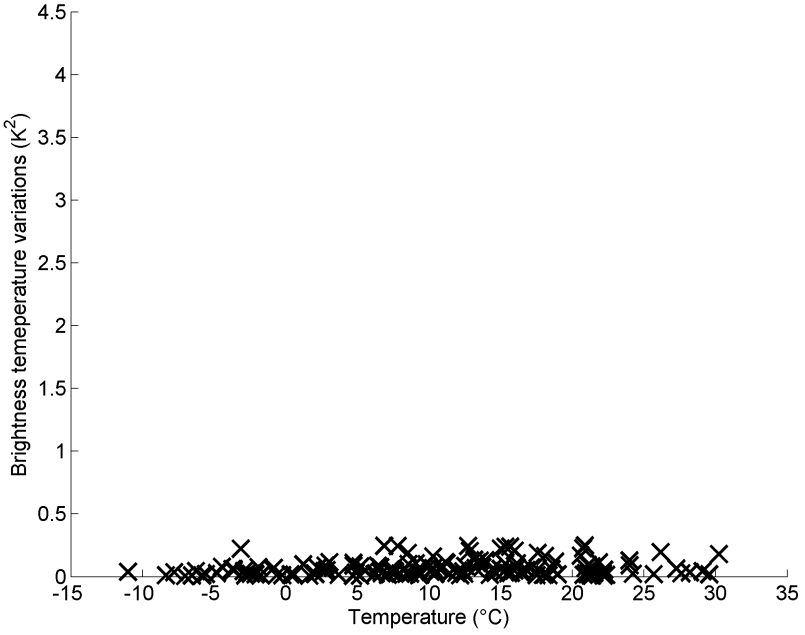

Figure 9: Brightness temperature variations when no clouds were present in the monitored volume of atmosphere.

The threshold of brightness temperature variations for the determination of cloud presence was parametrically determined as 0.23 K. Using this value as a decision-making parameter, the following results listed in Tab. 3 for temperatures higher than 0 °C were obtained from an analysis of 14 months of measurement data (314 captured events). The hit rate of estimates is substantially higher than the hit rate of estimates calculated for ambient temperatures below 0 °C, when the method cannot be properly applied. In such cases the hit rate was only 31.43 %.

Table 3: Hit rate of cloudiness forecasting when the temperature was higher than 0 °C.

		Event forecast	
		Yes	No
Event Observation	Yes	80.5 %	4.8 %
	No	14.7 %	–

WORKING METHODS: Fire Sensing Methodology

Principles of remote sensing of the atmosphere and ground are very well described. The fire-endangered environment is scanned by several means using different frequency bands. The basic observation in the visible light spectrum (450-750 nm) is the most inherent for human beings but has some complications. Just the visible part of fire can be seen and in most cases direct flames can be seen and detected. Such observation can be useless in case of obstacles that covers the area of interest or when the fire is in the smoldering phase and has no apparent fire signs. The last argument can be eliminated by using the thermal scanning (1400nm) but still there is a problem with obstacles. Since the microwave radiation can pass natural obstacles it is the reasonable choice to use microwave band as a next means for scanning.

Theoretical Introduction and Analysis of Fire Sensing

Since fire remote sensing is, by necessity, a down-looking application several effects must be taken into account. The ground surface is not an ideal environment in terms of microwaves propagation. There are many obstacles and inhomogeneities. Fires that should be detected can be easily overlooked in a tangle of vegetation, sand, wet and dry soil, etc. In addition, the emissivity of the sensed surface must be taken into account. Even the sky's reflection has a minor influence on the measurement and cannot be neglected. The derivation is well documented in [16].

A general scenario of spot sensing is depicted in Fig. 10. In this case no fire is present in the sensed spot.

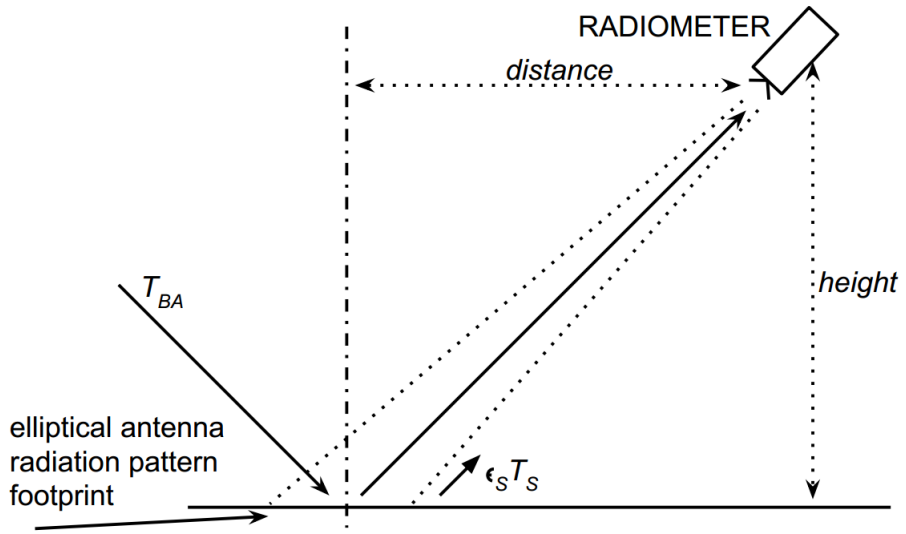

Figure 10: General remote sensing deployment focused on a ground target

The antenna is placed in a particular height. In this case the sensed temperature consists of two parts - the soil radiation and the reflected sky radiation. The part of brightness temperature that comes from soil is weighted by the soil emissivity. Likewise, the downward radiation is weighted by the ground reflectivity:

$$T_A = T_S\epsilon_S + (1-\epsilon_S)(T_{BA} + T_C e^{-\tau_{\upsilon,\infty}}), \tag{1}$$

where T_S stands for the soil thermodynamical temperature, ϵ_S is the emissivity of the soil and the right part of the formula represents downward atmospheric radiation T_{BA} and cosmic radiation background (T_{BC}) weighted by the soil reflectivity $(1-\epsilon_S)$.

Soil Emissivity

For early simulations the emissivity described in [17] was used. The emissivity of soil with low vegetation and X-band frequency is in the range from 0.92 to 0.95, it depends on the soil water content and surface roughness.

First experimental measurement was done within the thesis in order to obtain the soil emissivity. For this purpose the thermodynamical temperature of soil was measured as well as the brightness temperature of sensed spot and sky brightness temperature. The soil emissivity can be derived as

$$\epsilon_S = \frac{T_A - (T_{BA} + T_C e^{-\tau_{\upsilon,\infty}})}{T_S - (T_{BA} + T_C e^{-\tau_{\upsilon,\infty}})}. \tag{2}$$

During the experiment the radiometer antenna was pointed to the sky under the same elevation angle that was then used for fire sensing but in the upward direction. This measured brightness temperature is the T_{BA} parameter. Then the antenna was turned to the fire spot (without the fire yet) and the brightness was recorded again. The calculated emissivity during the period of several minutes is depicted in Fig. 11 . The measurement should take only a short time in order to avoid weather changes, clouds movements and fast environmental changes that can affect the measurement.

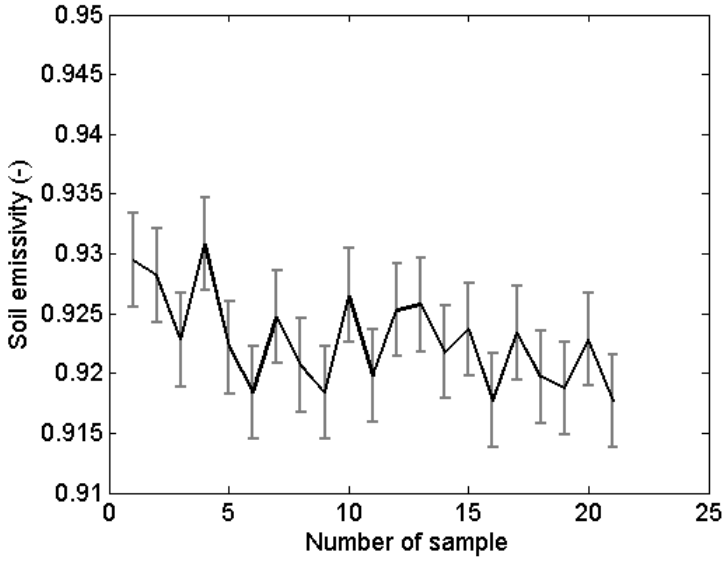

Figure 11: Soil emissivity measurement with marked standard deviation.

The experiment was done during cloudy day when the whole sky was covered by consistent altostratus cloud. The brightness temperature measured when pointing to the sky was in the range of 53 K to 55 K, soil thermodynamical temperature was in the range of 20 to 21 °C (293 – 294 K). Brightness temperature recorded by the radiometer was in the range of 273 to 277 K.

Filling Factor

For the radiometric measurement in relation with sensing of a bounded spot the filling factor quantity is generally used. It is a representative parameter of spatial resolution of the radiometric system. Usually the filling factor is considered as a fraction of the area covered by the fire which is seen by a radiometer. By using the filling factor the problem with sensing of same fire spot from various distances and under various angles is solved.

Generally the filling factor definition is understood as the power received from a bounded source in relation of the source at the same brightness temperature but filling the whole antenna radiation pattern [18, 19, 20].

Formally the filling factor can be calculated by

$$q = \frac{G_0}{4\pi} \iint\limits_{\Omega_F} F_n(\Theta, \varphi) d\Omega, \tag{3}$$

where G_0 stands for the antenna gain in the direction of maximum radiation, F_n is the normalized power radiation pattern and Ω_F means the spatial angle in which the fire spot is detectable by the antenna.

This equation can be successfully used for environment with more sources of radiation: fire, soil self-radiation, sky reflection etc.

For most cases the simple expression of filling factor can be used

$$q = \frac{A_F}{A_{ant}}, \tag{4}$$

where A_F stands for the area of fire and the A_{ant} is the antenna radiation pattern footprint restricted by the half-power beam-width.

Fire Emissivity

In order to supplement general knowledge about the fire sensing, the fire emissivity has to be found. When using approach by [20] the radiometric contrast of a fire spot and bare soil can be defined as

$$\rho_T = (1-\rho_V)(1-\rho_A)[\epsilon_F T_F - \epsilon_S T_S - (\epsilon_F - \epsilon_S)\epsilon_V T_V]q, \tag{5}$$

where $(1-\rho_V)$ is the transmissivity of vegetation that can cover the fire spot, $(1-\rho_A)$ is the transmissivity of atmosphere, ϵ_F, ϵ_S, ϵ_V stands for the fire emissivity, soil and vegetation respectively. T_F, T_S and T_V are the thermodynamical temperatures of corresponding objects.

Considering that no vegetation was over the fire spot and transmissivity of atmosphere of 1 the relation (5) can be simplified as

$$\rho_T = (\epsilon_F T_F - \epsilon_S T_S)q \tag{6}$$

and the fire emissivity can be expressed as

$$\epsilon_F = \frac{\frac{\rho_T}{q} + \epsilon_S T_S}{T_F}. \tag{7}$$

Since the soil emissivity can be measured as well as the soil and fire temperature the fire emissivity is an accessible number. In chapters – this relation is used for emissivity calculation. Also all scenarios were numerically simulated in MATLAB where the thermodynamical temperature of all objects, known emissivities and environmental parameters were taken into account. The simulation result is mentioned in following chapters as well.

RESULTS: Fire Sensing Methodology

Fire Detectability

In this chapter the detectability of a fire by a microwave radiometer is investigated. Simulations of several scenarios and together with outdoor measurement were performed in order to confirm detectability of the fire of specific temperature distributions and dimensions. Various scenarios for fire sensing were numerically modeled and simulated. Real parameters of antenna radiation pattern and radiometer sensitivity were taken into account. The concept of fire detectability verification was tested on real measurement data and then applied in a large scale on analyses of scaled airborne sensing of an environment. The results clearly indicate the possibilities and limits of detection with currently available radiometers.

The brightness temperature was calculated in simulations' stage by

$$T_A = \frac{1}{\Omega_A} \oiint_{4\pi} F_N(\Theta,\varphi) T_B(\Theta,\varphi) d\Omega, \tag{8}$$

where T_A is the antenna detected noise temperature, F_N represents the normalized antenna radiation pattern and T_B stands for the brightness temperature at given azimuth Θ and elevation φ angles.

In the following chapters several types of fires were measured in order to obtain the emissivity of various burning matter.

Airborne Sensing

When the wild fires are monitored it is usually done by remote sensing, mainly in the IR range and, experimentally, in a microwave band. In both cases airborne sensing is frequently used. At the start of our analysis a feasibility study of fire detectability by airborne sensing was done and the entire scenario was numerically simulated then downscaled to dimensions that are possible to measure in a

natural environment by the available measuring system, it was measured and the model was verified. The down scaled scenario is described in the following sections.

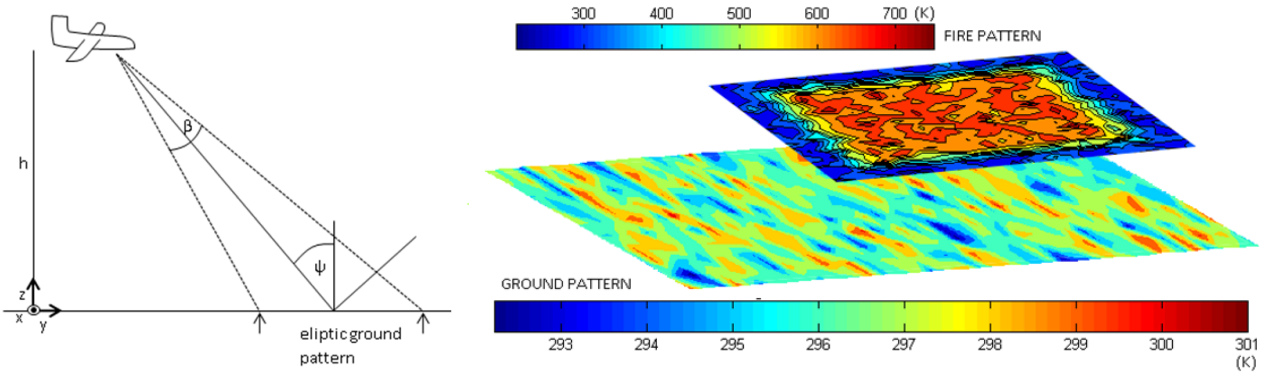

(a) (b)

Figure 12: Scenarios schemes: a) General schematic view; b) fire and ground temperature pattern (fire pattern is depicted in reduced scale).

Various scenarios have been analyzed. Typical scanning scene is depicted in Fig. 12a . Let us assume the ground is being sensed by an airborne radiometer at 300 m above ground level, with an incident angle (ψ) up to 45° in the forward direction of the track. In that case, the ground area scanned by antenna beam has an elliptical pattern. For analyses we assumed the ground plane area 500 m × 2400 m (width × length) with a resolution of 0.5 m/pixel. The analyzed fire was located from small scales up to 2/3 of the ground plane length.

Numerical analysis of the above mentioned scenario was performed to define the basic task of airborne sensing. Results from the analysis are shown in Fig. 13 .

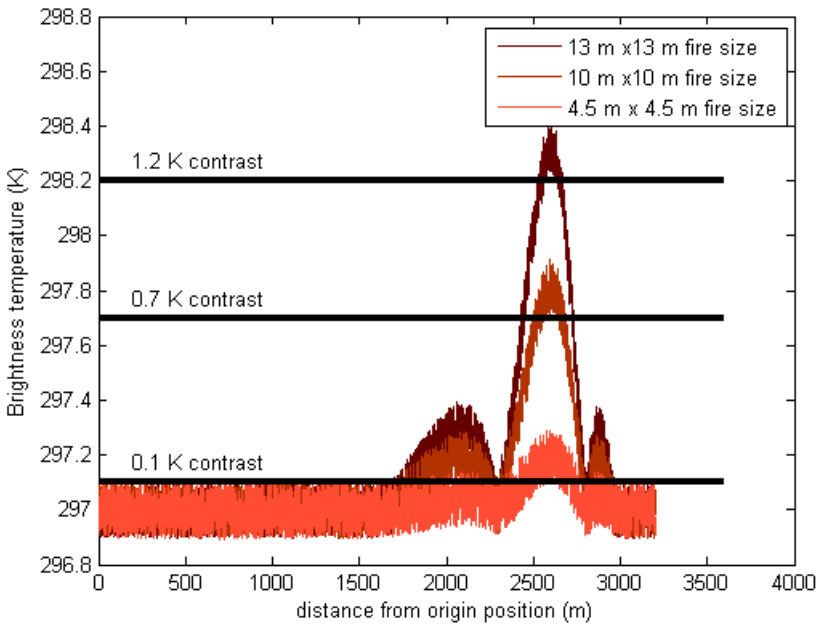

Figure 13: Three fires with different size at the temperature in the range of 220 - 290 °C.

The brightness temperature in the simulation was calculated by equation (8). Several fire types were analyzed. Results in this thesis are demonstrated on an example of the fire TF1 standardized in EN54, Part 9 [21] (burning cellulose wood, size 50 × 50 cm).

Fire in the first smoldering stage having the temperature in the range 220 to 290 °C was assumed. In this analysis 3 radiometers were considered: i) state-of-the-art radiometer [7], ii) commercially

available radiometer [22], and iii) radiometer from our laboratory [23]. Main results of the analysis reveal the fire dimensions that are still detectable with the mentioned instruments.

The results from analysis – the limits in microwave radiometer detection of fire – are shown in Table 4. Three values of radiometer sensitivity were used to verify detectability of the fire. The first one is for case of the state of the art radiometer with sensitivity 0.1 K [7], the second one for the commercially available radiometer [9] having sensitivity of 0.7 K and the third one representing the Dicke-type radiometer available in our laboratory with sensitivity of 1.2 K [23].

Table 4: Detectable fires sizes with respect to radiometer sensitivity.

			Event forecast		
Dimensions of fire (m × m)	Temperature of fire (°C)	Brightness temperature contrast (K)	State-of-art radiometer	Commercial radiometer	Radiometer at CTU lab
4.5 × 4.5	220-290	0.11	YES	NO	NO
10 × 10	220-290	0.72	YES	YES	YES
13 × 13	220-290	1.23	YES	YES	YES
4 × 4	300-350	0.13	YES	NO	NO
9.5 × 9.5	300-350	0.71	YES	YES	YES
11 × 11	300-350	1.35	YES	YES	YES

The influence of the fire area brightness temperature distribution was considered as well as various ground plane temperature distribution. Derived results can help hardware designers of radiometric instruments to design a receiver for the purpose of fire sensing with properly set sensitivity with respect to other radiometer potentially adjustable parameters (integration time).

Simulation of the above described scenario was done at first, and then it was verified by the measurement.

Gasoline Fire

The first fire studied was the gasoline fire. 100 cc of gasoline was absorbed into a cotton fabric. Size of the fabric was 50 × 50 cm. By the fabric it is preserved the fire size, shape and homogeneous gasoline distribution in the sensed area. Time of the whole measurement was approximately 11 minutes. In Figure 14 the course of the burning is depicted in series of 4 pictures.

Figure 14: Burning of the gasoline fire in 4-picture time series. Fire size 50 × 50 cm.

In Figure 15 the measured brightness temperature in a time series is depicted. The ignition occurred in the 7th minute and the whole combustion took approximately 2 minutes.

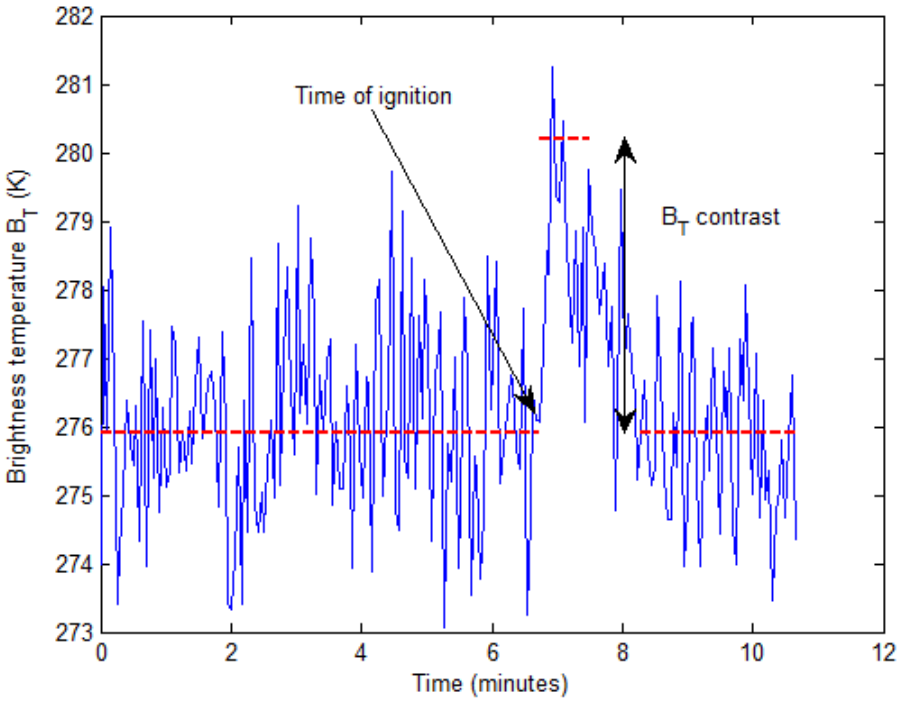

Figure 15: Gasoline fire microwave signature. Fire size 50 × 50 cm.

The fire place emissivity, the filling factor and other parameters can be calculated from the known parameters. A list of measured and calculated values is seen in Table 5.

Table 5: Gasoline fire measured parameters.

Parameter	Value
T_B (soil)	276.1 K
T_B (fire)	280.2 K
T_S	294 K
T_F	∼1220 K
ρ_T	4.1 K
ϵ_F (simulation)	0.247
ϵ_S	0.92
ϵ_F (measurement)	0.248
q	13.9 %

Where T_B (fire) is the averaged maximum brightness temperature measured during the burning process, ϵ_F (simulation) stands for the fire emissivity that was numerically simulated and ϵ_F (measurement) means the fire emissivity that was calculated from measurement by (7).

Wood Fire

In Figure 16 the measured brightness temperature of a wood cellulosic fire in a time series is depicted.

Figure 16: Burning of the wood cellulosic fire in 4-picture time series. Fire size 50 × 50 cm.

The ignition occurred in 4th minute – the first signal drop is apparent and it is caused by a worker who started the fire. Next, the fire was twice checked – the drop in 8th minute and 10th minute, caused again by a worker. These artificial influences were removed from dataset.

From the know parameters fire place emissivity, the filling factor and other parameters can be calculated. List of measured and calculated values is in Table 6.

Table 6: Wood fire measured parameters.

Parameter	Value
T_B (soil)	277.1 K
T_B (fire)	280.1 K
T_S	294 K
T_F	∼1200 K
ρ_T	4 K
ϵ_F (simulation)	0.252
ϵ_S	0.93
ϵ_F (measurement)	0.257
q	13.9 %

In Figure 17 the microwave signature of the wood fire is depicted.

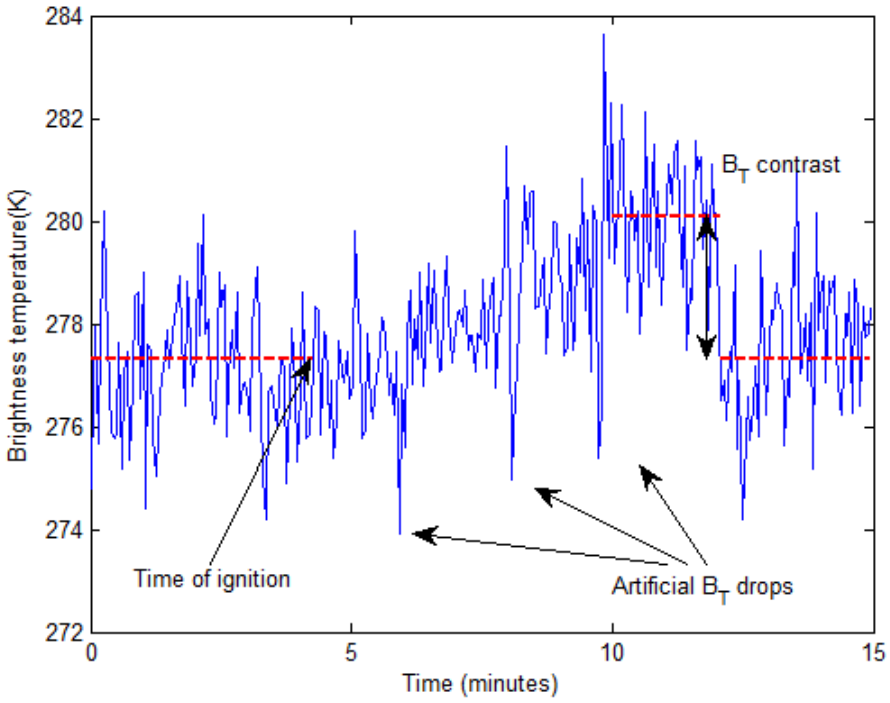

Figure 17: Wood fire microwave signature. Fire size 50 × 50 cm.

Straw Fire

In order to measure a well burning material with rapid ignition the straw fires were recorded. Those fires were measured with bigger fire spot in order to measure with various filling factor.

The straw fire example had size of 50 cm in the square shape. More amount of straw was used in order to spread it over the whole spot, approximately 600 g of dry straw was used. In Figure 18 the fire spot is depicted during the burning process.

Figure 18: Burning of the straw fire in 4-picture time series. Fire size 60 × 60 cm.

Since the straw fire was the biggest one, the highest radiometric brightness temperature contrast was recorded and very clear microwave signature of the fire was measured – see the signal in Fig. 19.

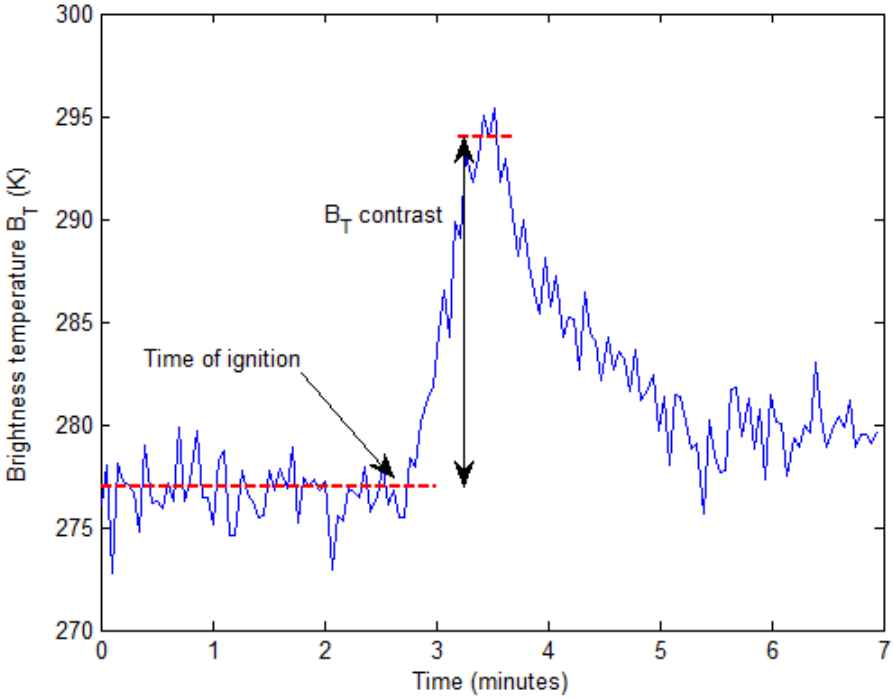

Figure 19: Straw fire microwave signature. Fire size 60 × 60 cm.

All important parameters of the straw measurement are listed in Table 7.

Table 7: Straw fire measured parameters. Fire size 60 × 60 cm.

Parameter	Value
T_B (soil)	277.2 K
T_B (fire)	294.9 K
T_S	294 K
T_F	$\sim$ 1420 K
ρ_T	17.7 K
ϵ_F (simulation)	0.255
ϵ_S	0.93
ϵ_F (measurement)	0.248
q	20.1 %

The possibility of the fire sensing by microwave radiometer has been verified via measurement campaign and several microwave fire signatures were determined. From the recorded and analyzed data the fire emissivity was calculated as a new crucial parameter. It has to be highlighted, to author knowledge this essential parameter has never been published or derived. The soil emissivity was measured as well in order to derive the radiometric background features beneath the fire. In following chapter the influence of fire size and temperature on radiometric contrast is measured and described to fulfill the methodology.

Fire Size and Temperature Influence

For the remote sensing of fire the influence of the fire size on the detectability is necessary to investigate as well as the fire temperature influence. The methodology of fire sensing is based on the different radiometric contrast caused by various fire temperature, size, emissivity of the places that are supposed to be sensed. In the following simulations and measurement both were investigated.

The same radiometric system as is described in chapter was used but the deployment of the radiometer and measured spot was different.

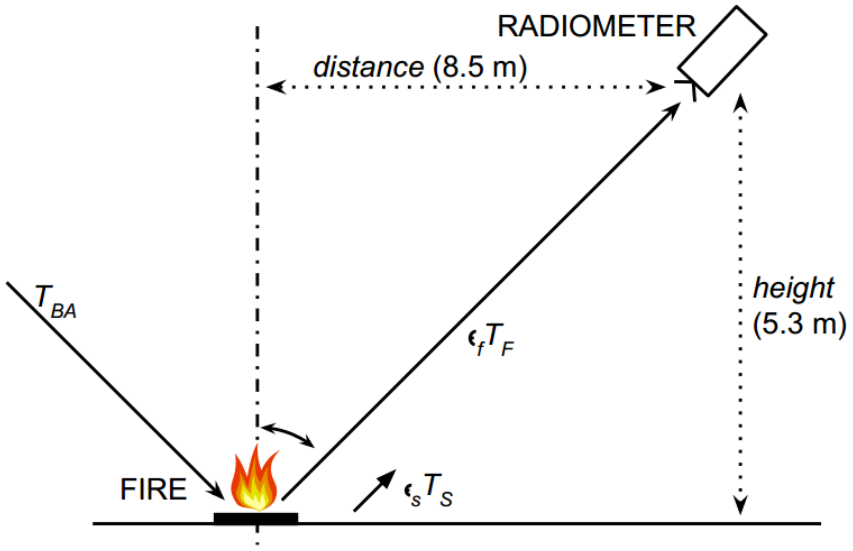

Figure 20: Fire measurement deployment.

For comparison purposes, an additional 2D-thermal fire sensing and scanning of surrounding temperature distribution was done by the FLIR i7 infrared camera [24].

A general scenario of simulations and measurement by the radiometer is depicted in Fig. 20. Such setup introduces typically used deployment for airborne sensing [25] so it is a good approximation of the up-scaled scenario. During the outdoor measurement the radiometer was placed in the height of 5.3 meters. The incident angle was 62°. Antenna was pointed to the center of fire area. The filling factor [16] in this case was about 15 %.

The same situation was numerically analyzed and the analogical numerical model was designed having resolution of 1 cm. The whole scenario was discretized and contribution of each cell to the total brightness temperature was taken into account. Every cell had a specific temperature and the antenna radiation pattern was involved in the simulation as well.

Fire size varied from the square area of 0.3 m × 0.3 m to 0.7 m × 0.7 m. Fire temperature varied in the range of 500 °C to approx. 1200 °C (due to the lower dynamic range of IR camera the upper temperature range was approximated).

Before the start of the first outdoor fire measurement, the brightness temperature background was sensed. The measured ground area had temperature distribution in the range of 5 to 15 °C. The soil was dry after a sunny day covered with grass. Figure 21 depicts sample of time series of measured and simulated data of brightness temperatures. The conditions of measurement were very steady, the brightness temperature of the background was stable more then 30 minutes.

For the first scenario a constant fire size was assumed and various temperatures were considered. The fire area had approximately square shape covering the size of 50 × 50 cm. The fire activated from glowing wooden sticks reached highs up to 2 m high having bright flames with the temperature approx. up to 1200 °C [21]. Fire development in time as caught by 4 IR shot sequences in 7 minutes is depicted in Figure 22 .

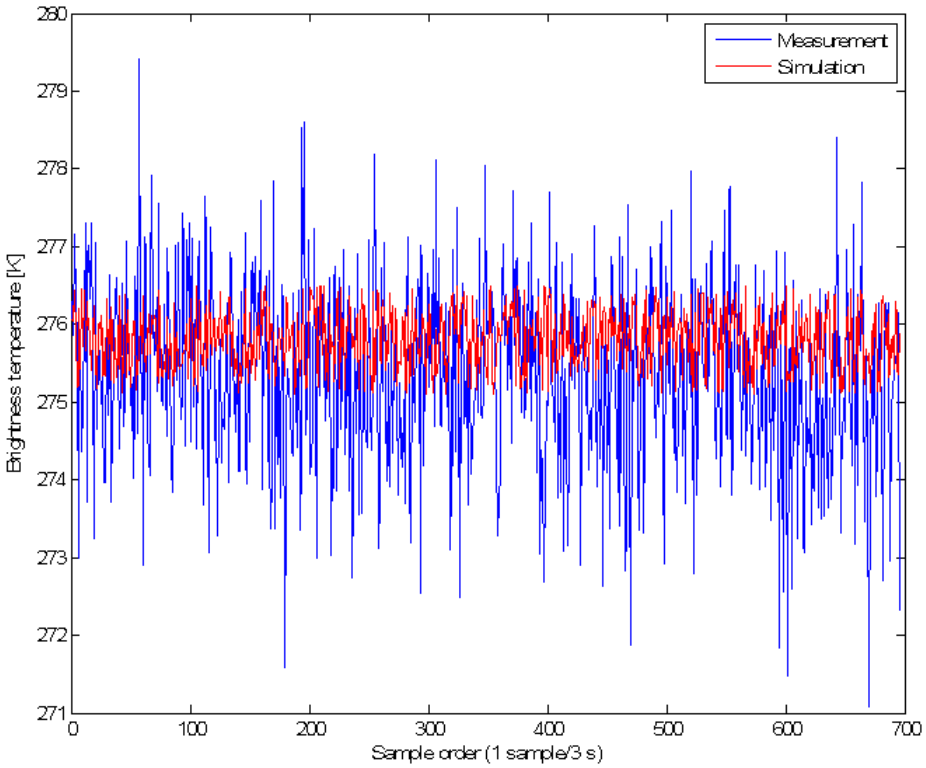

Figure 21: Measured background brightness temperature.

Figure 22: Fire development captured by the thermo-camera, temperature range is estimated up to approx. 1200 °C.

Recorded brightness temperature with dependence on fire temperature is in Figure 23.

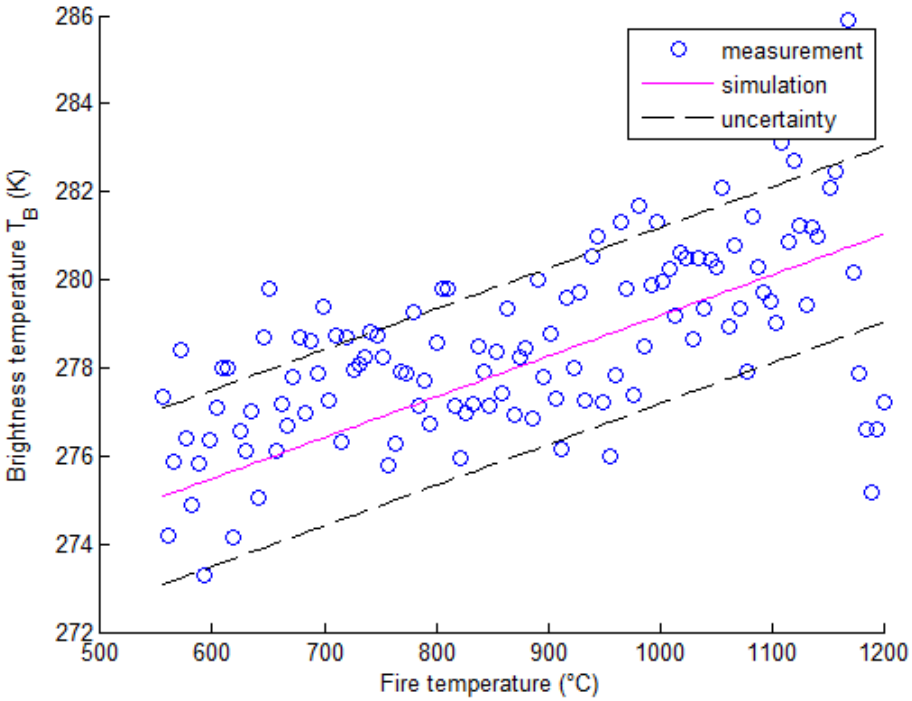

Figure 23: Measured brightness temperature as a dependency on fire temperature.

The fire temperature was activated by a compressed air and checked by the IR camera. Unfortunately, the low dynamical range of the available camera couldn't provide accurate values of the temperature so in later stages the temperature was estimated.

Second measurement was performed to capture brightness temperature as a dependency on fire size. The fire had a square shape varying from the size from 0.3 m × 0.3 m to 0.7 m × 0.7 m. Temperature of the fire was kept constant and was in the range of 500 to 600 °C. For this measurement only glowing charcoals were used in order to easily manipulate with the hot material. Measured values are shown in Figure 24.

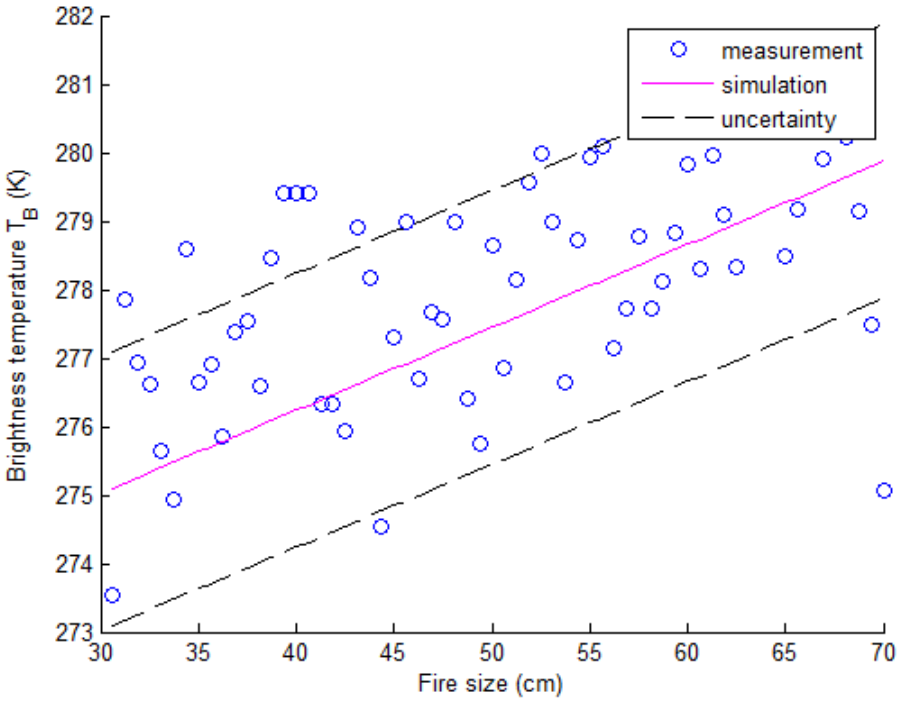

Figure 24: Measured brightness temperature as a function of fire size (x-axis describes length of edge of the square fire area).

In this case the resolution of numerical model was set to 10 cm per pixel (the smallest fire pixel size was assumed to be 10 × 10 cm). In the first approach, the model of fire had set constant temperature 550 °C (for distances and deployment see section the picture of deployment above). Results of analysis in terms of the dependency of fire size on brightness temperature contrast are described in Table 8.

Table 8: Dependency of demanded radiometer sensitivity on the fire size to be detected.

Fire temperature (°C)	Fire dimensions (cm)	Brightness temperature contrast (K)
550	10 × 10	0.17
550	20 × 20	0.69
550	50 × 50	4.29
550	100 × 100	16.76

Let us assume the ground without a fire has homogeneous temperature distribution. Once the lobe of antenna scans the fire area, the brightness temperature swell is recorded. Table 8 then distinguishes which fire size is detectable by specified brightness temperature contrast. For instance the brightness temperature contrast of fire having size of 10 × 10 cm is approximately 0.17 K. So the minimal radiometer sensitivity for detection such fire has to be at least 0.17 K as well. Next simulated scenario was analyzed to obtain the dependence for possibly measured contrasts of brightness temperatures under various fire temperatures. In this case the fire was set constant with size of 50 cm × 50 cm. The corresponding results of analysis are depicted in Table 9.

Table 9: Dependency of demanded radiometer sensitivity on the fire temperature to be detected.

Fire temperature (°C)	Fire dimensions (cm)	Brightness temperature contrast (K)
550	50 × 50	4.29
600	50 × 50	5.06
800	50 × 50	8.21
1000	50 × 50	11.35

For example for the size of mentioned fire with a temperature 550 °C is the brightness temperature contrast approximately 4 K. By the methodology of the fire sensing sensitivity with respect to the fire size it is necessary to involve in measurement a radiometer with the sensitivity of 4 K at least.

Methodology of Fire Sensing

The fire sensing is a complex task and the final measured brightness temperature depends on many effects which should be taken into account. During an on site measurement environmental parameters plays a significant role and must be known as well as the technological constraints of used radiometric system.

In order to sense a possible fire in the field the environmental parameters should be known. As the first step of the methodology the soil properties are necessary to consider. From the radiometric remote sensing point of view it is essential to know the soil emissivity or emissivity of any other natural background. How to measure it is described in chapter . The emissivity can vary from 0.8 to 0.95 and it is different for various vegetation types, sand, soil any other material and also depends on humidity etc.

Once the soil emissivity is known the limiting fire parameters must be found. In chapter a possible scenarios are listed. Fire sizes and its temperature influence on the detectability by a microwave radiometer are described with proposal of the minimal sensitivity which must be met. In Fig. 25 the dependency of fire temperature and its emissivity on the detectable radiometric contrast is depicted.

Radiometer sensitivity is the next parameter which is crucial for radiometric sensing of any objects. When this parameter can be chosen (during the instrumentation development) the choice must be based on the sensitivity study described above and in [26].

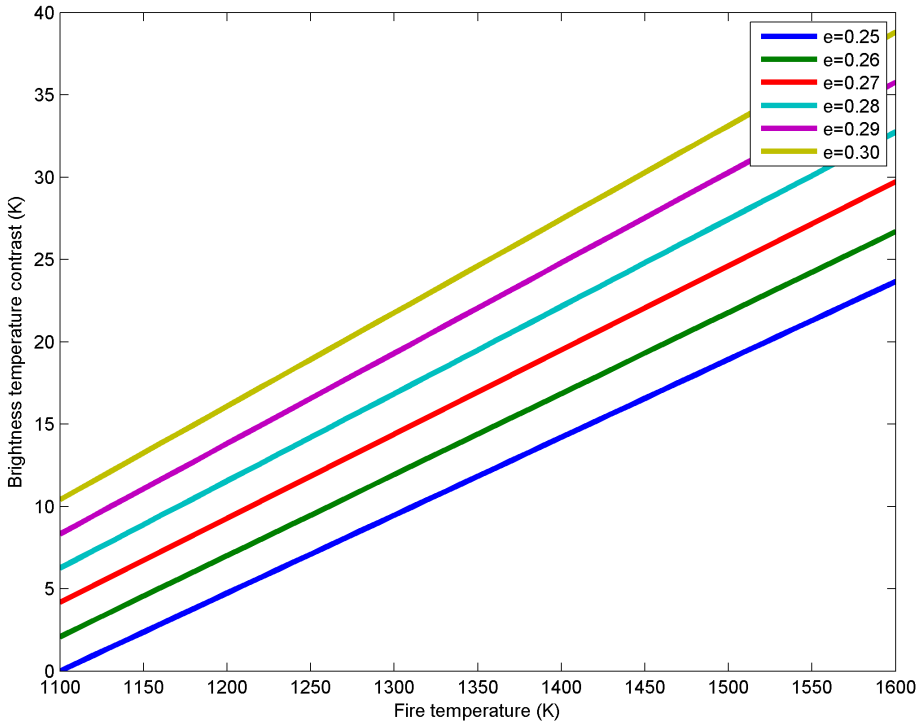

Figure 25: Radiometric contrast as a dependence on fire temperature and fire emissivity.

There are several ways for wild fire detection but the airborne sensing is the most convenient way in order to cover an extensive area in a short time. The last parameter is necessary to know and to set: filling factor as is described in chapter . The filling factor has significant influence on the possibility of fire detection. From Figure 26 the dependency of filling factor of fire with certain temperature is depicted.

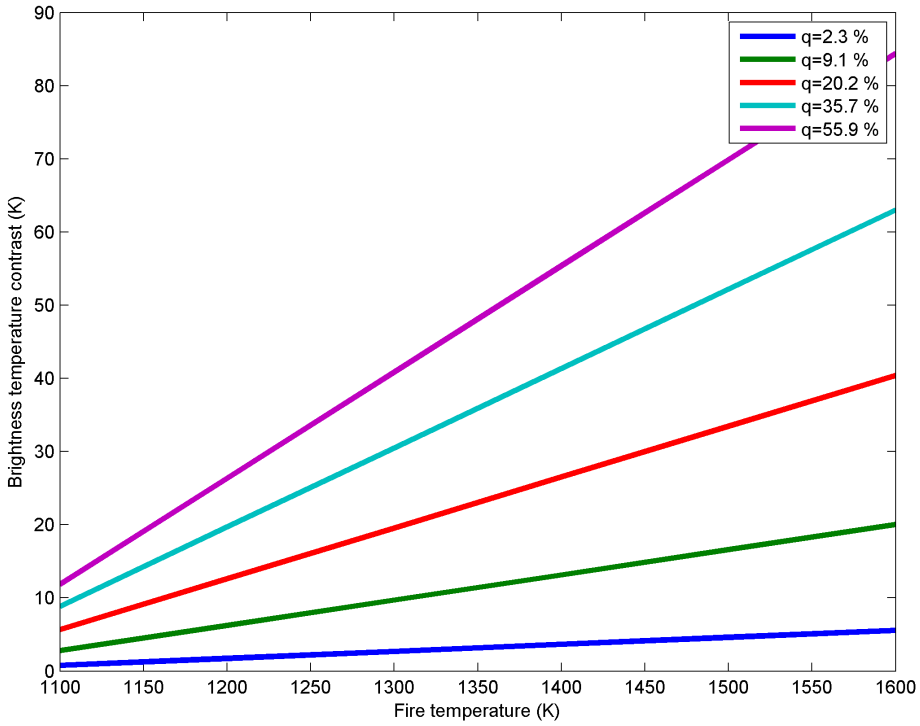

Figure 26: Radiometric contrast as a dependence on fire temperature and the filling factor.

When the radiometric system sensitivity is given and the fire temperature is known or expected it is possible to calculate the filling factor in order to plan e.g. altitude of the radiometer position as:

$$q = \frac{\rho_T}{(\epsilon_F T_F - \epsilon_S T_S)} \tag{9}$$

the ρ_T stands for the demanded brightness temperature or the radiometer sensitivity respectively.

CONCLUSION

The thesis was focused on methodologies of remote sensing by the microwave radiometer which allow improving current possibilities of rain prediction, cloud detection and fire sensing.

The first main aim was focused on the new methodology for rain prediction and cloud now-casting using a microwave radiometer. In the datasets, hundreds of atmospheric events was recorded and analyzed in order to propose methodology for rain forecasting. Several approaches were tested and finally the method for detection of the initial brightness temperature swell was derived. For the rain prediction the variance of brightness temperature is calculated over a short time window in order to get a trigger signal on the initial brightness temperature swell before the rain. As the decision making parameter the specific threshold for triggering before rain event was found by the parametric study and set to the threshold 10 K. This value gives the best results with the hit rate of 74.4 % with false alarms in 7.7 % of cases and the miss rate is 17.9 %. The best average forecasting time is 1.8 minutes which was achieved with respect to the low number of false alarms and missed events but expands even up to 10 min before rain (with acceptable hit rate). For the cloud detection the methodology of the brightness temperature variance over a longer time window was proposed and validated by further use of the radiometer. Utilizing the low threshold of 0.23 K in order to detect the cloudiness precise results were achieved and the cloudiness was detected with success rate better the 80 %. The influence of the ambient temperature on the detectability of clouds was investigated as well. Both methods were published in [14].

The second part of the thesis deals with so far not fully mature detection of fires by the microwave radiometer (minimum papers published worldwide). The requirement was to detect the fire by brightness temperature contrast. Since the soil, vegetation, human body and fire have significant difference of microwave emissivity the new methodology was analyzed based on the specific features of this parameter. The soil emissivity was measured in order to capture behavior of the radiometric background beneath the fire. Values in the range from 0.92 to 0.93 were obtained. Several measurements under natural conditions were performed to explore the microwave signatures of various fire types (cellulose, gasoline, straw, trash) and to derive the best possible approach. Value of the fire emissivity has been selected as the new key parameter which has not been investigated yet. The fire emissivity was determined by measurements and simulations to be in the range from 0.25 to 0.30 and this value was incorporated to the methodology. Influence of the fire size and temperature on the recorded brightness temperature contrast respectively was explored. All the results are described in the general form in order to allow choosing the proper radiometer for demanded purpose so the new methodology can be applicable for different equipments and under diverse conditions. Both the state-of-the-art as well as the commercially available instruments have been taken into account in order to ascertain the best achievable results with available instrumentation. Based on the measured data, calculated and derived results the simulations the new methodology of fire sensing was validated.

References

[1] Planck Collaboration I. Planck Early Results: I. The Planck mission. *Astronomy and Astrophysics*, 536(A1), June 2011. 16464.

[2] L. Terenzi, , M. Lapolla, M Laaninen, P. Battaglia, F. Cavaliere, A. De Rosa, N. Hughes, P. Jukkala, V.-H. KilpiA, G. Morgante, M. Tomasi, J. Varis, M Bersanelli, R. C. Butler, F. Ferrari, C. Franceschet, P. Leutenegger, N. Mandolesi, A. Mennella, R. Silvestri, L. Stringhetti, J. Tuovinen, L. Valenziano, and F. Villa. Cryogenic Environment and Performance for Testing the Planck Radiometers. *Journal of Instrumentation*, 4(12), December 2009. DOI 10.1088/1748-0221/4/12/T12015.

[3] J. Gueldner and D. Spankuch. Results of Year-Round Remotely Sensed Integrated Water Vapor by Ground-Based Microwave Radiometry. *Journal of Applied Meteorology*, 38:981–988, July 1999. ISSN 1520-0450.

[4] H. Y. Won, Yeon-Hee Kim, and Hee-Sang Lee. An Application of Brightness Temperature Received from a Ground-based Microwave Radiometer to Estimation of Precipitation Occurrences and Rainfall Intensity. *Asia-Pacific Journal of Atmospheric Sciences*, 45(1):55–69, 2009.

[5] Y. A. Hussin. MODIS - Moderate Resolution Imaging Spectro-Radiometry For Forest Detection. In *NEP-ITC RS/GIS for Monitoringand Assessment of Iraqi Marshland*, pages 1–27, Enschede, The Netherlands, 6-10 February 2005. United Nations Environment Programme.

[6] F. Alimenti, T. Kempka, G. Tasselli, S. Bonafoni, P. Basili, L. Roselli, K. Solbach, and H. I. Willms. Fire detection by low-cost microwave radiometric sensors. In *Microwave Radiometry and Remote Sensing of the Environment, 2008. MICRORAD 2008*, pages 1–4, Firenze, Italy, 11-14 March 2008. ISBN 978-1-4244-1986-9.

[7] F. Alimenti, D. Zito, A. Boni, M. Borgarino, A. Fonte, A. Carboni, S. Leone, M. Pifferi, L. Roselli, B. Neri, and R. Menozzi. System-on-chip microwave radiometer for thermal remote sensing and its application to the forest fire detection. In *15th IEEE International Conference on Electronics, Circuits and Systems, 2008. ICECS 2008.*, pages 1265–1268, St. Julien's, Malta, 31 August - 3 September 2008. ISBN 978-1-4244-2181-7.

[8] G. Tasselli, F. Alimenti, A. Fonte, D. Zito, L. Roselli, D. De Rossi, A. Lanata, B. Neri, and A. Tognetti. Wearable microwave radiometers for remote fire detection: System-on-Chip (SoC) design and proof of the concept. In *Engineering in Medicine and Biology Society, 2008. EMBS 2008. 30th Annual International Conference of the IEEE*, pages 981–984, Vancouver, BC, Canada, August 2008. DOI 10.1109/IEMBS.2008.4649319.

[9] N. Skou and D. Le Vine. *Microwave Radiometer Systems: Design and Analysis*. Artech House Inc., Norwood, Massachusetts, USA, 2 edition, 2006. ISBN 1-58053-974-2.

[10] E. A. Sharkov. *Passive Microwave Remote Sensing of the Earth*. Books in geophysical science. Praxis Publishing Ltd., Chichester, UK, 1 edition, December 2009. ISBN 3540439463A.

[11] Anemo s.r.o. *WS981 (manual)*. Anemo s.r.o., Jana Masaryka 26, Prague, Czech Republic, August 2011. [Online; accessed 11-June-2013], Available at http://www.anemo.cz/dokumenty/WS981navod.zip.

[12] R. R. Ferraro, E. A. Smith, W. Berg, and G. J. Huffman. A Screening Methodology for Passive Microwave Precipitation Retrieval Algorithms. *Journal of the Atmospheric Sciences*, 55(9):1583–1600, May 1998. ISSN 0022-4928.

[13] G. M. Skofronick-Jackson, A. J. Gasiewski, and J. R. Wang. Influence of microphysical cloud parameterizations on microwave brightness temperatures. *IEEE Transactions on Geoscience and Remote Sensing*, 40(1):187–196, January 2002. DOI 10.1109/36.981360.

[14] World Meteorological Organization (WMO). *Guide to Meteorological Instruments and Methods of Observation*. Number 8 in Instruments and Methods of Observation Programme (IMOP). World Meteorological Organization, Geneva, Switzerland, 7 edition, 2008. ISBN 978-92-63-10008-5.

[15] D. G. Long, Q. P. Remund, and D. L. Daum. A cloud-removal algorithm for SSM/I data. *IEEE Transactions on Geoscience and Remote Sensing*, 37(1):54–62, January 1999. ISSN 0196-2892.

[16] G. Tasselli, F. Alimenti, S. Bonafoni, P. Basili, and L. Roselli. Fire Detection by Microwave Radiometric Sensors: Modeling a Scenario in the Presence of Obstacles. *IEEE Transactions on Geoscience and Remote Sensing*, 48(1):314–324, January 2010. DOI 10.1109/TGRS.2009.2024305.

[17] S. Paloscia. Contribution of Microwave Radiometry in Agrometeorological Studies. In *EARSEL Advances in Remote Sensing*, volume 2 of *2*, pages 15–21, June 1993. ISBN 2908885069.

[18] P. F. Goldsmith, C. T. Hsieh, G. R. Huguenin, J. Kapitzky, and E. L. Moore. Focal Plane Imaging Systems for Millimeter Wavelengths. *IEEE Transactions on Microwave Theory and Techniques*, 41(10):1664–1675, October 1993. ISSN 0018-9480.

[19] P. F. Goldsmith. *Quasioptical Systems:Gaussian Beam Quasioptical Propogation and Applications*, volume 4. Wiley-IEEE Press, 1 edition, December 1997. ISBN 0780334396.

[20] G. Luzzi, P. Ferrazzoli, S. Gagliani, and T. Mazzoni. *Microwave Radiometry and Remote Sensing of The Environment*, chapter Microwave radiometry as a tool for forest fire detection: Model analysis and preliminary experiments, pages 411–418. Utrecht: VSP, Rome, Italy, February 1994. ISBN 90-6764-189-9.

[21] European Committee for Standardization. EN 54-9 Components of Automatic Fire Detection Systems - Methods of Test of Sensitivity to Fire. EN Standard BS 5445-9:1984, EN 54-9:1982, British Standards Institution, May 1982. ISBN 0-580-13876-3.

[22] I. PopStefanija. Airborne L-band Radiometers for Remote Sensing of Soil Moisture. Commercial product datasheet, ProSensing Inc., Amherst, USA, 2012. [Online; accessed 3-July-2013], Available at http://www.northerngulfinstitute.org/ noaa_uas_wksp_2012/presentations/ PopStefanija_AirborneL-bandRadiometers.pdf.

[23] P. Dvorak, M. Mazanek, and S. Zvanovec. Short-term Prediction and Detection of Dynamic Atmospheric Phenomena by Microwave Radiometer. *Radioengineering*, 21(4):1060–1066, 2010. ISSN: 1210-2512.

[24] Inc. FLIR Systems. FLIR i-Series Infrared Camera Comparison Chart., 2013. [Online; accessed 19-June-2013], Avilable at http://www.flir.com/thermography /americas/us/view/?id=54156&collectionid=601& col=54163?

[25] F. T. Ulaby, R. K. Moore, and A. K. Fung. *Microwave Remote Sensing, Active and Passive*, volume 1 of *Microwave Remote Sensing Fundamentals and Radiometry*. Artech House Inc., Norwood, Massachusetts, USA, March 1981. ISBN 0-89006-190-4.

[26] P. Dvorak and S. Zvanovec. On the Sensitivity of Fire Detection by a Microwave Radiometer. In *IEEE International Geoscience and Remote Sensing Symposium*, pages 402–405, Melbourne, Australia, July 21-26 2013. IEEE Geoscience and Remote Sensing Society. ISBN 978-1-4799-1113-4.

Publikace vztahující se k tématu disertační práce

Publikace v impaktovaných časopisech:

Petr Dvorak (33 %), Milos Mazanek, Stanislav Zvánovec. Short-term Prediction and Detection of Dynamic Atmospheric Phenomena by Microwave Radiometer. Radioengineering. 2012, vol. 21, no. 4, p. 1060-1066. ISSN 1210-2512.
Citováno: bez citace

Petr Dvorak (50 %), Stanislav Zvanovec. On the sensitivity of Fire Detection by a Microwave Radiometer. IEEE Geoscience and Remote Sensing Letters. Submitted for review. 2014.

Publikace v recenzovaných časopisech

Patenty

Petr Dvorak (50 %), Jiri Libich. Diferenciální teplotní senzor. [Funkční vzorek]. 2010.

Publikace excerpované WOS

Petr Dvorak (33 %), Jiri Libich, Stanislav Zvanovec. Combined Measured Characteristics of Microwave Radiometer and Free-Space Optical Link, IEEE AP-S/URSI Conference - Paper #2121. 26-30 Mar 2012.

Publikace ostatní:

Petr Dvorak (50 %), Stanislav Zvanovec. On the Sensitivity of Fire Detection by a Microwave Radiometer, IEEE International Geoscience and Remote Sensing Symposium, Melbourne, Australia,. Vol. 3, pp.402-405.4, 21-26. July 2013.

Jiri Libich, Martin Mudroch, Petr Dvorak (25 %), Stanislav Zvanovec, „Performance Analysis of Hybrid FSO/RF Link" EuCAP 2012: the 6th Conference on Antennas and Propagation, Prague, 2012.

Petr Dvorak (25 %), Federico Alimenti, Paolo Mezannotte, Luca Roselli. 31.4GHz BEOL Embedded BiCMOS MEMS Switch, Barcelona, Spain /7th MC Meeting and Workshop of COST IC0803, September 19, 2011.

Petr Dvorak (100 %), Radiometer Based Subsystem for On-line Atmosphere Monitoring 5th Management Committee/Working Group Meeting and Workshop - November 8-9, 2010, Ecole Polytechnique Fédérale de Lausanne, CH-105 Lausanne, Switzerland

Publikace ostatní

Publikace v impaktovaných časopisech:

Jiri Libich, Petr Dvorak (25 %), Petr Piksa, Stanislav ZVANOVEC, „Correction of Thermal Deviations in Fabry-Perot Resonator Based Measurements of Specific Gases in Millimeter Wave Bands“, Radioengineering, 2012, vol. 21, no. 1, p. 459-463. ISSN 1210-2512.

Publikace v recenzovaných časopisech

Patenty

Publikace excerpované WOS

Publikace ostatní

Procentuální podíl všech spoluautorů u uvedených publikací je rovnoměrný.

Summary

In this thesis new methodologies of remote sensing from the radiometric point of view will be described. The main thesis focus consists of two parts, the first part deals with the new methodology of atmosphere dynamic effects (rain, clouds) sensing. The methodology is based on evaluation of brightness temperature variance. Next, methodology of fire remote detection and it's properties from the microwave point of view is proposed. Fire emissivity, other properties and environmental parameters are examined and described.

Keywords: radiometry, atmosphere sensing, rain prediction, fire sensing.

Resumé

V teto dizertační tezi jsou popsány nové metodiky dálkového průzkumu z pohledu radiometrie. Hlavní práce je složena ze dvou částí. První část popisuje novou metodiku měření atmosférických dynamických jevů (deště, oblačnost). Metodika je založena na vyhodnocení rozptylu měřené jasové teploty. V druhé části je navržena nová metodika dálkové detekce ohně na základě mikrovlnných vlastností prostředí a samotného ohně. Všechny tyto parametry a vlastnosti jsou prozkoumány a popsány.

Keywords: radiometrie, průzkum atmosféry, předpověd deště, detekce ohně.